

SegRet: An Efficient Design for Semantic Segmentation with Retentive Network

Zhiyuan Li¹, Yi Chang^{1,2,3}, Yuan Wu^{1*}

¹School of Artificial intelligence, Jilin University

²Engineering Research Center of Knowledge-Driven Human-Machine Intelligence, Jilin University

³International Center of Future Science, Jilin University

zhiyuanl24@mails.jlu.edu.cn, {yichang, yuanwu}@jlu.edu.cn,

Abstract

With the ongoing advancement of autonomous driving technology and intelligent transportation systems, research into semantic segmentation has become increasingly pivotal. Accurate understanding and analysis of real-world scenarios are now essential for these emerging fields. However, traditional semantic segmentation methods often struggle to balance high model accuracy with computational efficiency, particularly in terms of parameter count. To address this challenge, we introduce SegRet, a novel approach that leverages the Retentive Network (RetNet) architecture and integrates a lightweight residual decoder featuring zero-initialization. SegRet exhibits three key characteristics: (1) Lightweight Residual Decoder: We incorporate a zero-initialization layer within the residual network framework, ensuring that the decoder remains computationally efficient while preserving critical information flow; (2) Robust Feature Extraction: Utilizing RetNet as the backbone, our model adeptly extracts hierarchical features from input images, thereby enhancing the depth and breadth of feature representation; (3) Parameter Efficiency: SegRet achieves state-of-the-art performance while significantly reducing the number of parameters, maintaining high accuracy without compromising on computational resources. Empirical evaluations on benchmark datasets such as ADE20K, Cityscapes, and COCO-Stuff10K demonstrate the efficacy of our approach. SegRet delivers impressive results, achieving an mIoU of 52.23% on ADE20K with only 95.81M parameters, 83.36% on Cityscapes, and 46.63% on COCO-Stuff. The code is available at: <https://github.com/ZhiyuanLi218/segret>.

1 Introduction

Semantic segmentation is the process of assigning semantic labels to each pixel in an image, enabling machines to perceive and understand scenes at the pixel level [Lateef and

Ruichek, 2019]. Tasks such as obstacle detection, lane tracking, and scene understanding rely crucially on the identification and description of elements such as roads, vehicles, pedestrians, and other objects of interest, especially for the safe and efficient operation of autonomous vehicles.

In recent years, deep learning-based methods have become the mainstream technology for semantic segmentation tasks. Classic semantic segmentation networks such as FCN [Long *et al.*, 2014], Mask R-CNN [He *et al.*, 2017], and PSPNet [Zhao *et al.*, 2017] have greatly propelled the development of semantic segmentation. With the successful applications of Transformers [Vaswani *et al.*, 2017] in NLP and CV domains, including models like ViT [Dosovitskiy *et al.*, 2021], SwinTransformer [Liu *et al.*, 2021], and DETR [Carion *et al.*, 2020], these networks have also been widely adopted as backbones for semantic segmentation. However, the computational complexity introduced by the self-attention mechanism poses significant challenges for Transformer-based semantic segmentation models. To address this issue, networks such as ReViT [Diko *et al.*, 2024], ExMobileViT [Yang *et al.*, 2023], and EfficientFormer [Li *et al.*, 2022] have been proposed.

Recently, various network architectures have been proposed to compete with Transformer, like Mamba [Gu and Dao, 2023], RWKV [Li *et al.*, 2024b], and RetNet [Sun *et al.*, 2023]. These new models have shown significant advantages over Transformers. Mamba achieves efficient processing of long sequences through linear time complexity and selective state space, and has been widely applied in tasks such as VMamba [Liu *et al.*, 2024b], VM-UNet [Ruan and Xiang, 2024], and RSMamba [Chen *et al.*, 2024a]. RWKV combines the characteristics of recurrent neural networks and transformers. By leveraging its novel recurrent weighted key-value mechanism, it enables efficient processing of sequential data and has been widely applied in the field of vision [Li *et al.*, 2024b]. While RetNet enhances inference efficiency and performance by simplifying the self-attention mechanism and introducing hidden fusion modules [Sun *et al.*, 2023].

Semantic segmentation networks typically adopt an encoder-decoder architecture, where the encoder extracts high-level feature representations from input images, and the decoder maps these features to pixel-level semantic labels for image segmentation. However, decoders often contain a large number of parameters, such as UperNet [Xiao *et al.*, 2018]

*Corresponding author

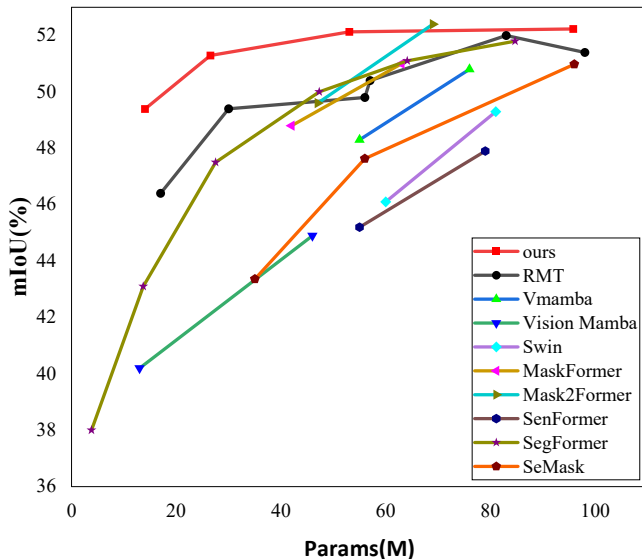


Figure 1: **Model comparison on ADE20K.** Multi-scale inference is used for all results. The proposed model achieves 52.23% mIoU.

and MaskFormer [Cheng *et al.*, 2021], posing challenges for semantic segmentation algorithms requiring real-time performance. Therefore, researchers are devoted to reducing parameter count, and improving inference speed, while maintaining or enhancing segmentation accuracy.

To address these challenges, we propose a novel method named SegRet. In the encoder section, SegRet uses Vision RetNet, which is pre-trained on ImageNet1K, as a hierarchical feature extractor. It extracts features across four different scales, ranging from low to high dimensions. In the decoder section, we have designed a lightweight residual connection decoder. The largest model decoder has only 2.6M parameters. We have introduced zero-initialized layers in the residual connection section to facilitate the fusion of hierarchical features. As shown in Figure 1, our approach captures hierarchical features from input images and reduces the model’s parameter count, achieving a balance between accuracy and efficiency. Evaluation results on benchmark datasets such as ADE20K [Zhou *et al.*, 2017], Cityscapes [Cordts *et al.*, 2016] and COCO-Stuff [Caesar *et al.*, 2018] demonstrate the effectiveness of our method, achieving high accuracy while reducing computational overhead. Specifically, our Tiny model achieves an mIoU score of 49.39 on the ADE20K dataset, 81.75 on the Cityscapes dataset and 43.32 on the COCO-Stuff dataset with only 14.01M parameters. On the other hand, the Large model, with 95.81M parameters, achieves an mIoU score of 52.23 on the ADE20K dataset, 83.36 on the Cityscapes dataset and 46.63 on the COCO-Stuff dataset.

This paper presents a novel semantic segmentation method, with the following main contributions:

- Vision RetNet is adopted as a hierarchical feature extractor, demonstrating the strong potential of RetNet in the field of semantic segmentation.
- A lightweight residual decoder is designed and zero initialization layers are introduced, achieving considerable

decoding capability with fewer parameters.

- Significant improvements in accuracy are achieved compared to recent studies while reducing parameter count.

2 Related Work

2.1 Semantic Segmentation.

Traditional semantic segmentation methods primarily rely on manually designed features and classifiers for pixel-level classification. These methods typically utilize low-level features such as color, texture, and shape, combined with algorithms like graph cuts and random forests for segmentation [Zheng *et al.*, 2012; Arbelaez *et al.*, 2010; Zhang *et al.*, 2016]. However, due to the complexity and variability of real-world situations, traditional methods often struggle to effectively handle issues such as occlusion and lighting variations, leading to inaccurate segmentation results.

With the application of deep learning to semantic segmentation tasks, the accuracy of semantic segmentation has been improved. These deep learning models achieve pixel-level to semantic-level mapping by introducing operations such as upsampling and skip connections, significantly enhancing the accuracy and efficiency of semantic segmentation [Paszke *et al.*, 2016; Yu *et al.*, 2017; He *et al.*, 2019a; He *et al.*, 2019b]. Recent models mostly rely on Transformer-based architectures, which introduce self-attention mechanisms to capture global dependencies among pixels in the image, thus better understand the semantic information within the images [Zheng *et al.*, 2021; Xie *et al.*, 2021; Cheng *et al.*, 2022; Zhang *et al.*, 2022]. The latest research combines zero-shot learning and prompt learning in semantic segmentation. This allows for the identification of new classes without annotated data and provides additional information to guide the model towards more precise segmentation. These methods demonstrate unique advantages in addressing data scarcity and improving model performance. [Kirillov *et al.*, 2023; Zhang *et al.*, 2023; Zhang *et al.*, 2024b].

2.2 State Space Model

Due to the unfriendliness of Transformer attention mechanisms to long text sequences, researchers have begun exploring new model architectures to overcome this challenge, where state space models like Mamba [Gu and Dao, 2023], DenseMamba [He *et al.*, 2024], and RetNet [Sun *et al.*, 2023] have garnered widespread attention. These models adopt mechanisms different from Transformer to process textual data, especially in handling long sequences, demonstrating higher efficiency and better performance.

Building on the success of state space models, researchers further apply them to the visual domain, proposing a series of visual models based on state space models. These models inherit the advantages of state space models in handling long sequences while incorporating the characteristics of visual data, effectively processing visual information such as images and videos. Among them, models like Vmamba [Liu *et al.*, 2024b], Vision Mamba [Zhu *et al.*, 2024], and Vision RetNet [Fan *et al.*, 2023] are widely used, excelling not only in tasks such as image classification and object detection but also providing new insights and methods for handling

complex visual scenes [Li *et al.*, 2024a; Liu *et al.*, 2024a; Chen *et al.*, 2024b].

3 Method

This section introduces the SegRet model, beginning with an overview of its core structure. Subsequently, we provide a detailed explanation of the Vision RetNet, which serves as a hierarchical feature extractor for effective feature representation. Finally, we conduct an in-depth analysis of the lightweight residual decoder, emphasizing its pivotal role in preserving model accuracy while minimizing the parameter count.

As shown in Fig 2, the SegRet model utilizes an encoder-decoder structure. The encoder utilizes Vision RetNet as a feature extractor to extract features at four different resolutions. Subsequently, these extracted features are fed into the residual decoder. The residual decoder consists of a linear mapping block and a zero-initialized residual block, which is mapped to a semantic segmentation mask after feature fusion.

3.1 Vision RetNet Backbone

RetNet

Firstly, we revisit the self-attention mechanism of the Transformer. For each input vector X , by multiplying matrices W_Q , W_K and W_V with X , we obtain the Q , K and V vectors respectively. Therefore, the self-attention is defined as:

$$\text{Attention}(Q, K, V) = \text{softmax}\left(\frac{QK^T}{\sqrt{d_k}}\right)V. \quad (1)$$

To address issues such as training parallelism, low-cost inference and performance optimization encountered by Transformers in large language models, the Retentive Network (RetNet) is proposed. RetNet, as a novel foundational architecture, theoretically derives the connection between recurrence and attention, and introduces a retention mechanism for sequence modeling, supporting three computational paradigms: parallel, recurrent, and block-recurrent.

The retention mechanism is the core of RetNet, with the following fundamental principles:

$$o_n = \sum_{m=1}^n \gamma^{n-m} (Q_n e^{in\theta}) (K_m e^{im\theta})^\dagger v_m, \quad (2)$$

where Q , K , and V vectors, similar to the Transformer, are obtained through affine transformations of input X .

Building upon this foundation, the parallel form is deduced as:

$$Q = (XW_Q) \odot \Theta, K = (XW_K) \odot \bar{\Theta}, V = XW_V, \quad (3)$$

$$\Theta_n = e^{in\theta}, D_{nm} = \begin{cases} \gamma^{n-m}, & n \geq m \\ 0, & n < m \end{cases}, \quad (4)$$

$$\text{Retention}(X) = (QK^T \odot D)V, \quad (5)$$

where Θ denotes its own complex conjugate, $D \in \mathbb{R}^{|x| \times |x|}$ represents causal masking and exponential decay, indicating relative distances within a one-dimensional sequence. The

outstanding performance, training parallelism, low-cost deployment, and efficient inference demonstrated by RetNet enable it to effectively address the issue of excessively high complexity in Transformers.

Vision RetNet

Vision RetNet [Fan *et al.*, 2023], is the earliest visual state space model designed as an alternative to Transformer. This model improves upon RetNet, particularly in modifying the matrix D for handling causal masking and exponential decay, transforming it from a unidirectional matrix suitable for NLP to a bidirectional matrix adapted for computer vision (CV) scenarios.

Formally, the BiRetention operator is defined as follows:

$$\text{BiRetention}(X) = (QK^T \odot D^{Bi})V, \quad (6)$$

$$D_{nm}^{Bi} = \gamma^{|n-m|}. \quad (7)$$

Specifically, for the two-dimensional spatial attributes of images, the matrix D is modified to its two-dimensional version to better capture spatial relationships, expressed as:

$$D_{nm}^{2d} = \gamma^{|x_n - x_m| + |y_n - y_m|}. \quad (8)$$

Moreover, due to the high resolution of visual images resulting in a large number of tokens, computational costs become prohibitively complex. To address this issue, Vision RetNet proposes a method of decomposing computations along both axes of the image. Specifically, attention mechanisms and distance matrices are computed separately in the horizontal and vertical directions to reduce computational complexity. The computational process is outlined as follows:

$$Q_H, K_H = (Q, K)^{B,L,C \rightarrow B,W,H,C}, \quad (9)$$

$$Q_W, K_W = (Q, K)^{B,L,C \rightarrow B,H,W,C}, \quad (10)$$

$$\text{Attn}_H = \text{Softmax}(Q_H K_H^T) \odot D^H, \quad (11)$$

$$\text{Attn}_W = \text{Softmax}(Q_W K_W^T) \odot D^W, \quad (12)$$

$$D_{nm}^H = \gamma^{|y_n - y_m|}, \quad D_{nm}^W = \gamma^{|x_n - x_m|}, \quad (13)$$

$$\text{ReSA}_{dec}(X) = \text{Attn}_H(\text{Attn}_W V)^T. \quad (14)$$

The proposed SegRet model consists of Vision RetNet, which combines the output features of RMT blocks after each downsampling step into hierarchical feature matrices and feeds them into the decoder for further processing.

3.2 Lighting residual decoder

At the current stage, most popular decoders are composed of complex CNN or Transformer structures, resulting in a large number of parameters and lacking real-time performance. To address this issue, we propose a lightweight residual decoder. As illustrated in Fig 2, the proposed decoder consists of only 2.6M parameters, primarily composed of two parts: a linear mapping block and a zero-initialized residual structure. The architecture of our decoder is presented as follows:

The input to the decoder is a list containing features from different layers, denoted as $Features = [f_1, f_2, \dots, f_n]$,

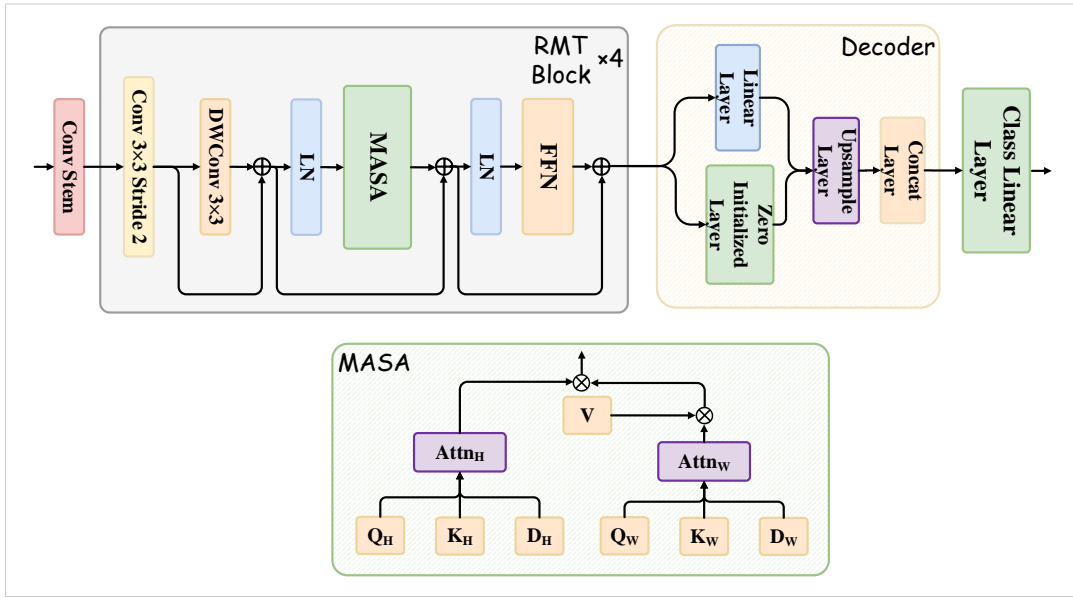


Figure 2: **An overview of the proposed SegRet model.** We use Vision RetNet as a hierarchical feature extractor to introduce RetNet into semantic segmentation for the first time (Section 3.1). For more efficient feature fusion, a zero-initialization residual decoder is applied to predict semantic segmentation masks (Section 3.2).

where f_i represents the feature from the i -th layer with varying channel sizes. The objective of the decoder is to integrate these features into the final output, which has dimensions $n_{cls} \times H \times W$, where n_{cls} is the number of classes, H and W are the height and width of the output image. The decoding process is represented as follows:

Initially, each input feature f_i undergoes a linear transformation to standardize its channel size to C , resulting in the transformed feature F_i . This process can be expressed as:

$$F_i = \text{Linear}(f_i). \quad (15)$$

We perform a residual connection between the original feature f_i and the transformed feature F_i . The residual connection layer is implemented using a 1×1 convolution with zero initialization, where the output feature map's channel size matches that of f_i . Specifically, the output of the residual connection layer can be represented as:

$$F'_i = f_i + \text{Zero-initialized Conv}(F_i), \quad (16)$$

where Zero-initialized Conv denotes a 1×1 convolution operation with zero initialization. All features F'_i are upsampled to $1/4$ of the image size. The upsampled feature can be represented as $\text{Upsample}(F'_i)$.

The upsampled features F'_i are concatenated to obtain the output image. Assuming the merged feature is M , the concatenation operation can be represented as:

$$M = \text{Concat}(\text{Upsample}(F'_1), \dots, \text{Upsample}(F'_n)). \quad (17)$$

The dimensions of M are $[4C, H, W]$. Finally, the merged feature M undergoes a linear mapping to adjust the channel size to the required number of classes n_{class} . This process can be expressed as:

$$\text{Output} = \text{Linear}(M). \quad (18)$$

4 Experiments

We compared recent research methods on the ADE20K, Cityscapes and COCO-Stuff datasets, demonstrating that our proposed SegRet model successfully integrates RetNet into the semantic segmentation domain. Through comparative evaluation of model parameters and mIoU metrics, our experiments confirm that SegRet is a powerful semantic segmentation approach.

Datasets ADE20K, Cityscapes and COCO-Stuff are important datasets in the field of semantic segmentation. ADE20K is a large-scale scene parsing dataset containing over 20,000 high-resolution images covering various scenes and environments. Each image is densely annotated with 150 different semantic categories, including objects, scenes, and parts. Cityscapes is a dataset focused on the understanding and analysis of urban scenes, comprising 5,000 high-resolution images from 50 cities in Germany. Each image provides detailed pixel-level annotations covering common semantic categories in urban scenes such as roads, vehicles, pedestrians and more, totaling 19 different semantic categories. COCO-Stuff10K is a subset of the Microsoft COCO dataset. The dataset comprises over 10,000 images, with each image annotated with 171 different categories, including common objects, scenes and backgrounds. COCO-Stuff10K boasts more detailed and refined annotations, making it an ideal benchmark for many image segmentation algorithms.

4.1 Implementation details

Based on considerations of the applicability of the model in different scenarios, we propose four models of different sizes:

Method	Backbone	Decoder head	Image Size	#params	mIoU(SS)	mIoU(MS)	FLOPs
SenFormer [Bousselham <i>et al.</i> , 2021]	R50		512*512	55M	44.4	45.2	179G
SenFormer [Bousselham <i>et al.</i> , 2021]	R101		512*512	79M	46.9	47.9	199G
SegFormer [Xie <i>et al.</i> , 2021]	MiT-B1		512*512	13.7M	42.21	43.1	15.9G
SegFormer [Xie <i>et al.</i> , 2021]	MiT-B2		512*512	27.5M	46.5	47.5	62.4G
Vision Mamba [Zhu <i>et al.</i> , 2024]	Vim-Ti	UperNet	512*512	13M	-	40.2	-
Vision Mamba [Zhu <i>et al.</i> , 2024]	Vim-S	UperNet	512*512	46M	-	44.9	-
SeMask [Jain <i>et al.</i> , 2023]	SeMask Swin-T	FPN	512*512	35M	42.06	43.36	40G
SeMask [Jain <i>et al.</i> , 2023]	SeMask Swin-S	FPN	512*512	56M	45.92	47.63	63G
Swin [Liu <i>et al.</i> , 2021]	Swin-T	UperNet	512*512	60M	-	46.1	236G
Swin [Liu <i>et al.</i> , 2021]	Swin-S	UperNet	512*512	81M	-	49.3	259G
RMT [Fan <i>et al.</i> , 2023]	RMT-T	FPN	512*512	17M	-	46.4	33.7G
RMT [Fan <i>et al.</i> , 2023]	RMT-S	FPN	512*512	30M	-	49.4	180G
SenFormer [Bousselham <i>et al.</i> , 2021]	Swin-T		512*512	59M	46	-	179G
MaskFormer [Cheng <i>et al.</i> , 2021]	Swin-T		512*512	42M	46.7±0.7	48.8±0.6	55G
Vmamba [Liu <i>et al.</i> , 2024b]	VMamba-T	UperNet	512*512	55M	47.3	48.3	939G
Mask2Former [Cheng <i>et al.</i> , 2022]	Swin-T		512*512	47M	47.7	49.6	74G
Ours-Tiny	RMT-T		512*512	14.01M	48.76	49.39	72.28G

Table 1: Comparison of the proposed SegRet-Tiny model on ADE20k val dataset. Compared to recent studies, our tiny model shows significant advantages in terms of number of parameters and mIoU. All FLOPs of our model are measured at a resolution of 512×2048 . "SS" and "MS" in the table represent single-scale and multi-scale inference, respectively, with the best results highlighted in bold.

Method	Backbone	Decoder head	Image Size	#params	mIoU(SS)	mIoU(MS)	FLOPs
SenFormer [Bousselham <i>et al.</i> , 2021]	R50		512*1024	55M	78.8	80.1	179G
SenFormer [Bousselham <i>et al.</i> , 2021]	R101		512*1024	79M	79.9	81.4	199G
ECFD-tiny [Zhang <i>et al.</i> , 2024a]	R50		512*1024	41M	79.91	81.18	206G
ECFD-small [Zhang <i>et al.</i> , 2024a]	R50		512*1024	51M	80.14	81.32	222G
ECFD-tiny [Zhang <i>et al.</i> , 2024a]	R101		512*1024	60M	80.5	81.48	245G
ECFD-small [Zhang <i>et al.</i> , 2024a]	R101		512*1024	70M	80.74	82	261G
SeMask [Jain <i>et al.</i> , 2023]	SeMask Swin-T	FPN	768*768	34M	74.92	76.56	84G
SegFormer [Xie <i>et al.</i> , 2021]	MiT-B1		1024*1024	13.7M	78.5	80	243.7G
Segmenter [Strudel <i>et al.</i> , 2021]	DeiT-B/16	Seg-B*/16	768*768	-	-	80.5	-
Segmenter [Strudel <i>et al.</i> , 2021]	DeiT-B/16	Seg-B*-Mask/16	768*768	-	-	80.6	-
Segmenter [Strudel <i>et al.</i> , 2021]	ViT-L/16	Seg-L/16	768*768	-	-	80.7	-
Segmenter [Strudel <i>et al.</i> , 2021]	ViT-L/16	Seg-L-Mask/16	768*768	-	79.1	81.3	-
Ours	RMT-T		512*1024	14.01M	81.75	82.17	72.28G

Table 2: Comparison of the proposed SegRet-Tiny model on Cityscapes dataset.

Method	Backbone	Decoder head	Image Size	#params	mIoU(SS)	mIoU(MS)
MaskFormer [Cheng <i>et al.</i> , 2021]	R50		640*640	-	37.1±0.4	38.9±0.2
SenFormer [Bousselham <i>et al.</i> , 2021]	R50		512*512	55M	40	41.3
SeMask [Jain <i>et al.</i> , 2023]	SeMask Swin-T	FPN	512*512	35M	37.53	38.88
APPNet [Zhu <i>et al.</i> , 2023]	HRNet-W48	APPNet+HRNet	520*520	69.7M	36.9	-
APPNet [Zhu <i>et al.</i> , 2023]	HRNet-W48	APPNet+OCR	520*520	72.3M	40.3	-
Ours	RMT-T		512*512	14.01M	42.22	43.32

Table 3: Comparison of the proposed SegRet-Tiny model on COCO-Stuff dataset.

Tiny, Small, Base, and Large. Our backbone adopts the same parameter settings as Vision RetNet and is pre-trained on the ImageNet1K dataset. The size of the hidden layer parameter C in the decoder is [256, 256, 256, 512] for the four sizes, respectively. The SegRet model is built on the mmsegmentation framework and trained on four Nvidia A40 GPUs. We randomly flip and crop the ADE20K and COCO-Stuff dataset to a size of 512×512 and perform the same operations on the

Cityscapes dataset, resulting in a size of 512×1024 . Specifically, on the ADE20K dataset, the Large model is randomly cropped to 640×640 . To ensure fairness, we did not use training strategies such as OHem. We utilized cross-entropy loss and the AdamW optimizer, with a learning rate of 0.0001 and weight decay of 0.01. The batch sizes for ADE20K and COCO-Stuff were set to 16, while Cityscapes was set to 8. ADE20K and Cityscapes were trained for 160k iterations,

and COCO-Stuff for 80k iterations. The evaluation process followed the same settings as Mask2former.

4.2 Main results

We quantitatively analyze SegRet’s results on ADE20K and CityScapes, showcasing its remarkable performance in semantic segmentation tasks.

ADE20K Table 1 demonstrates the comparison between SegRet-Tiny and recent studies in terms of parameter count and mIoU. The results reveal that SegRet achieves state-of-the-art performance compared to models with similar parameter counts, with only 14.01M parameters yielding a 49.39 mIoU. For instance, compared to Mask2Former(Swin-T), we achieve comparable results with less than one-third of the parameters. Contrasting with Vision Mamba (Vim-Ti) with a similar parameter count, SegRet outperforms it by 9.7% in mIoU. Other model results at different scales are detailed in the Appendix.

Cityscapes As shown in Table 2, our SegRet-Tiny model shows satisfactory performance on the Cityscapes dataset. Compared to methods such as EFCD (EFCD-Small) and SegFormer (MiT-B1), SegRet achieves significant improvements in mIoU(SS) and mIoU(MS) with comparable parameter counts, reaching 81.75% and 82.17%, respectively. Compared to models such as SeMask and ECFD (EFCD-Large), SegRet achieves higher scores in mIoU(MS) with half the number of parameters, indicating superior generalization ability in multi-scale scenarios. Other model results at different scales are detailed in the Appendix.

COCO-Stuff The proposed SegRet-Tiny model demonstrates significant performance advantages on the COCO-Stuff dataset. As shown in Table 3, compared to other state-of-the-art methods such as MaskFormer, SenFormer, SeMask, and APPNet, our model achieves higher mIoU scores in image segmentation tasks. Specifically, our model achieves mIoU scores of 42.22 and 43.32 under single-scale (SS) and multi-scale (MS) evaluations, respectively. This indicates that our SegRet-Tiny model exhibits competitive advantages in both parameter efficiency and performance. Other model results at different scales are detailed in the Appendix.

Qualitative analysis As shown in Figure 3, we conducted a qualitative analysis on the ADE20K validation set. Our Tiny model was compared extensively with the MaskFormer (Swin-T) model. The results indicate that our proposed model outperforms MaskFormer significantly in handling details and error classification. This notable advantage is attributed to the powerful feature extraction capability of Vision RetNet and the more concise and effective decoder structure we proposed.

4.3 Ablation Studies

In this section, we conducted a series of ablation experiments to validate the effectiveness of the proposed decoder residual structure, particularly focusing on the validation of zero-initialized residual layers. Additionally, we delved into the analysis of the impact of decoder hidden layer parameters C on the experimental outcomes. All experiments were conducted on the ADE20K dataset.

Zero-initialized residual layer In Table 4, we investigated the impact of adding and removing zero-initialized residual(ZIR) layers on the proposed decoder. Our experiments were conducted on SegRet-Small with all settings consistent with formal training. We observed that adding the ZIR Layer led to a 0.79% increase in mIoU while only increasing parameters by 0.25M. This indicates the effectiveness of the SegRet structure.

Method	ZIR Layer	#params	mIoU(SS)
SegRet-Small	✓	26.27M	49.9
		26.52M	50.69

Table 4: Influence of zero-initialized residual layers on the Proposed Model

The impact of decoder hidden layer parameter C We investigated the impact of decoder hidden layer parameter C on the performance of the proposed model. The results from Table 5 indicate that as parameter C increases, the model’s performance also improves. Specifically, when C is set to 512, the model achieves the highest mean Intersection over Union (mIoU). However, when C is increased to 768, both the model’s complexity and mIoU are lower compared to the case when C is 512. Therefore, in our formal experiments, we adopted parameter C values of 256 (in the Tiny, Small, and Base models) and 512 (in the Large model).

Method	C	#params	mIoU(SS)
	256	94.26M	50.9
SegRet-Large	512	95.81M	52
	768	98.54M	51.57

Table 5: The Impact of Decoder Hidden Layer Parameter C on the Proposed Model

Input Scaling We conducted input scaling experiments using the CityScapes dataset. The findings indicate that varying input image sizes has a notable impact on the performance of the semantic segmentation model. As shown in Figure 4, across input images of four distinct dimensions (512x1024, 768x768, 640x1280, and 1024x1024), our model consistently demonstrated superior performance compared to alternative models, exhibiting higher mean Intersection over Union (mIoU) scores. It is notable that our model achieved optimal performance when the input image size was set to 1024x1024, attaining the highest mIoU of 82.02%. Furthermore, our model demonstrated commendable performance metrics while maintaining a modest parameter count of 14.01M, thus underscoring its efficacy in achieving parametric efficiency.

5 Conclusion

We propose SegRet, a semantic segmentation model that utilizes Vision RetNet and a zero-initialized residual decoder. This model introduces RetNet into the semantic segmentation

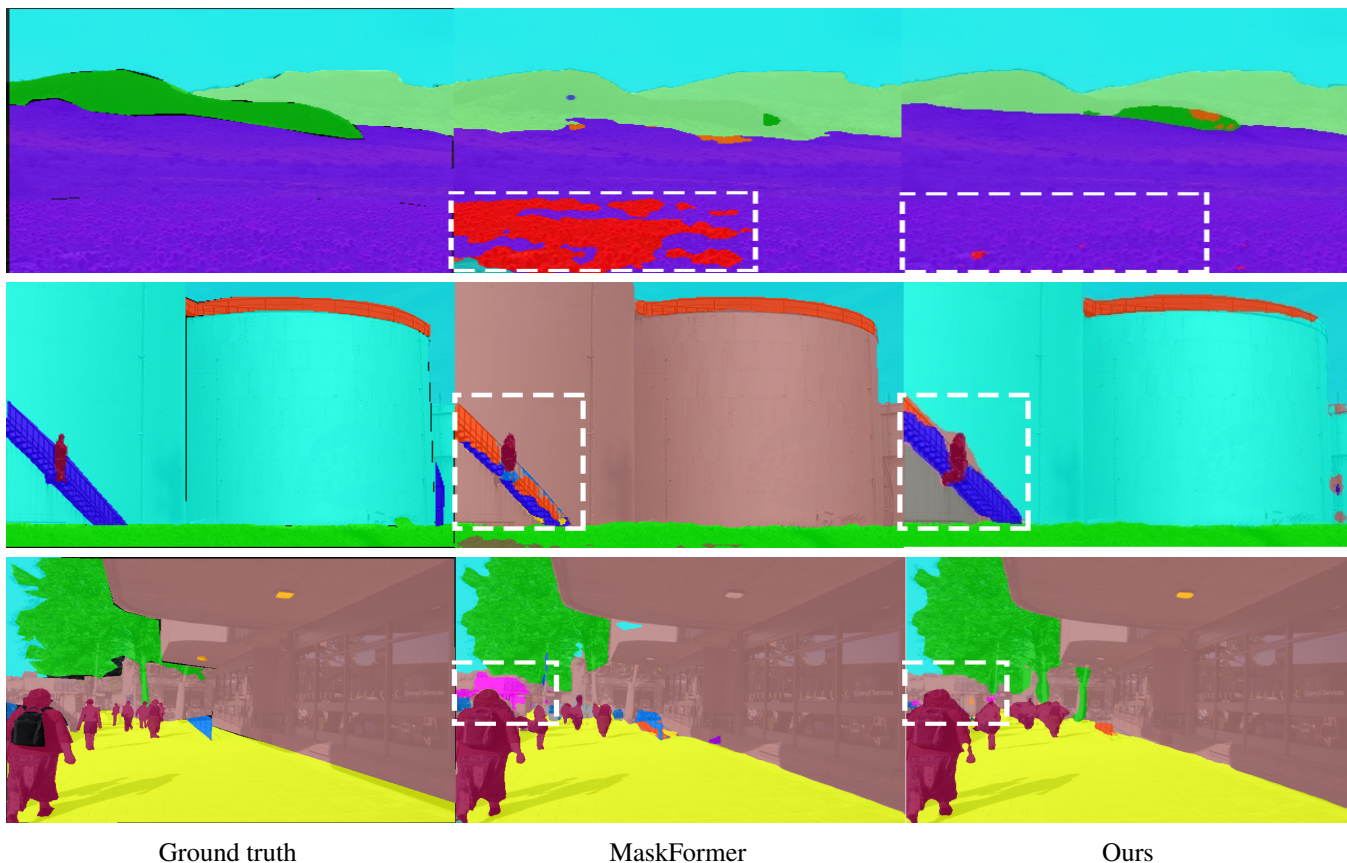


Figure 3: **Qualitative analysis is conducted on the ADE20K validation set.** The first column displays the ground truth values, while the outputs of MaskFormer and our proposed model are presented in the second and third columns, respectively. MaskFormer uses Swin-T as its backbone, while our model utilizes the RMT-T backbone.

field for the first time and incorporates zero-initialized layers into the residual connections of the decoder. Experimental results demonstrate that SegRet effectively maintains or improves accuracy while reducing parameter count, achieving excellent performance on four sizes of models across two datasets. However, SegRet’s current limitation is its inability to achieve satisfactory results in tasks such as medical image segmentation and remote sensing image segmentation. We anticipate that RetNet will further demonstrate greater performance in the visual domain.

References

- [Arbelaez *et al.*, 2010] Pablo Arbelaez, Michael Maire, Charless Fowlkes, and Jitendra Malik. Contour detection and hierarchical image segmentation. *IEEE transactions on pattern analysis and machine intelligence*, 33(5):898–916, 2010.
- [Bousselham *et al.*, 2021] Walid Bousselham, Guillaume Thibault, Lucas Pagano, Archana Machireddy, Joe Gray, Young Hwan Chang, and Xubo Song. Efficient self-ensemble for semantic segmentation. *arXiv preprint arXiv:2111.13280*, 2021.
- [Caesar *et al.*, 2018] Holger Caesar, Jasper Uijlings, and Vittorio Ferrari. Coco-stuff: Thing and stuff classes in context. In *Proceedings of the IEEE conference on computer vision and pattern recognition*, pages 1209–1218, 2018.
- [Carion *et al.*, 2020] Nicolas Carion, Francisco Massa, Gabriel Synnaeve, Nicolas Usunier, Alexander Kirillov, and Sergey Zagoruyko. End-to-end object detection with transformers. In *European conference on computer vision*, pages 213–229. Springer, 2020.
- [Chen *et al.*, 2024a] Keyan Chen, Bowen Chen, Chenyang Liu, Wenyuan Li, Zhengxia Zou, and Zhenwei Shi. Rs-mamba: Remote sensing image classification with state space model. *arXiv preprint arXiv:2403.19654*, 2024.
- [Chen *et al.*, 2024b] Tianxiang Chen, Zhentao Tan, Tao Gong, Qi Chu, Yue Wu, Bin Liu, Jieping Ye, and Nenghai Yu. Mim-istd: Mamba-in-mamba for efficient infrared small target detection. *arXiv preprint arXiv:2403.02148*, 2024.
- [Cheng *et al.*, 2021] Bowen Cheng, Alex Schwing, and Alexander Kirillov. Per-pixel classification is not all you need for semantic segmentation. *Advances in neural information processing systems*, 34:17864–17875, 2021.

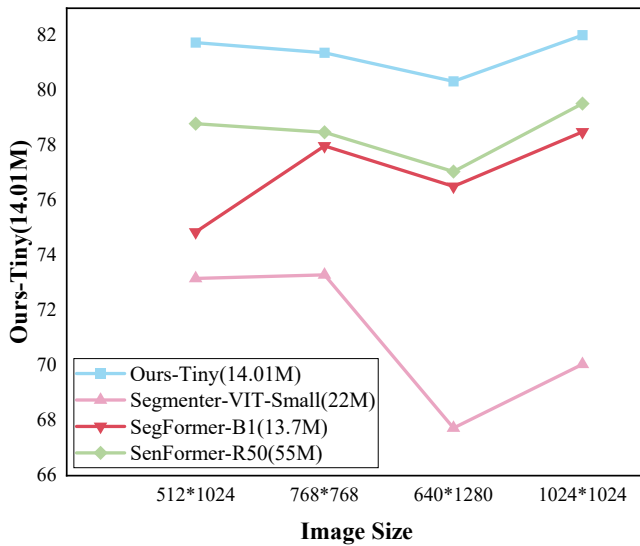


Figure 4: **A Comparative Study of scaling Input Sizes on Cityscapes.** We examined the impact of four different input dimensions (512*1024 to 1024*1024) on the model’s accuracy.

[Cheng *et al.*, 2022] Bowen Cheng, Ishan Misra, Alexander G Schwing, Alexander Kirillov, and Rohit Girdhar. Masked-attention mask transformer for universal image segmentation. In *Proceedings of the IEEE/CVF conference on computer vision and pattern recognition*, pages 1290–1299, 2022.

[Cordts *et al.*, 2016] Marius Cordts, Mohamed Omran, Sebastian Ramos, Timo Rehfeld, Markus Enzweiler, Rodrigo Benenson, Uwe Franke, Stefan Roth, and Bernt Schiele. The cityscapes dataset for semantic urban scene understanding. In *Proceedings of the IEEE conference on computer vision and pattern recognition*, pages 3213–3223, 2016.

[Diko *et al.*, 2024] Anxhelo Diko, Danilo Avola, Marco Cascio, and Luigi Cinque. Revit: Enhancing vision transformers with attention residual connections for visual recognition. *arXiv preprint arXiv:2402.11301*, 2024.

[Dosovitskiy *et al.*, 2021] Alexey Dosovitskiy, Lucas Beyer, Alexander Kolesnikov, Dirk Weissenborn, Xiaohua Zhai, Thomas Unterthiner, Mostafa Dehghani, Matthias Minderer, Georg Heigold, and Sylvain Gelly. An image is worth 16x16 words: Transformers for image recognition at scale. In *International Conference on Learning Representations*, 2021.

[Fan *et al.*, 2023] Qihang Fan, Huaibo Huang, Mingrui Chen, Hongmin Liu, and Ran He. Rmt: Retentive networks meet vision transformers. *arXiv preprint arXiv:2309.11523*, 2023.

[Gu and Dao, 2023] Albert Gu and Tri Dao. Mamba: Linear-time sequence modeling with selective state spaces. *arXiv preprint arXiv:2312.00752*, 2023.

[He *et al.*, 2017] Kaiming He, Georgia Gkioxari, Piotr Dollár, and Ross Girshick. Mask r-cnn. *IEEE Transactions on Pattern Analysis & Machine Intelligence*, 2017.

[He *et al.*, 2019a] Junjun He, Zhongying Deng, and Yu Qiao. Dynamic multi-scale filters for semantic segmentation. In *Proceedings of the IEEE/CVF international conference on computer vision*, pages 3562–3572, 2019.

[He *et al.*, 2019b] Junjun He, Zhongying Deng, Lei Zhou, Yali Wang, and Yu Qiao. Adaptive pyramid context network for semantic segmentation. In *Proceedings of the IEEE/CVF conference on computer vision and pattern recognition*, pages 7519–7528, 2019.

[He *et al.*, 2024] Wei He, Kai Han, Yehui Tang, Chengcheng Wang, Yujie Yang, Tianyu Guo, and Yunhe Wang. Densemamba: State space models with dense hidden connection for efficient large language models. *arXiv preprint arXiv:2403.00818*, 2024.

[Jain *et al.*, 2023] Jitesh Jain, Anukriti Singh, Nikita Orlov, Zilong Huang, Jiachen Li, Steven Walton, and Humphrey Shi. Semask: Semantically masked transformers for semantic segmentation. In *Proceedings of the IEEE/CVF International Conference on Computer Vision*, pages 752–761, 2023.

[Kirillov *et al.*, 2023] Alexander Kirillov, Eric Mintun, Nikhila Ravi, Hanzi Mao, Chloe Rolland, Laura Gustafson, Tete Xiao, Spencer Whitehead, Alexander C Berg, Wan-Yen Lo, et al. Segment anything. In *Proceedings of the IEEE/CVF International Conference on Computer Vision*, pages 4015–4026, 2023.

[Lateef and Ruichek, 2019] Fahad Lateef and Yassine Ruichek. Survey on semantic segmentation using deep learning techniques. *Neurocomputing*, 338:321–348, 2019.

[Li *et al.*, 2022] Yanyu Li, Geng Yuan, Yang Wen, Ju Hu, Georgios Evangelidis, Sergey Tulyakov, Yanzhi Wang, and Jian Ren. Efficientformer: Vision transformers at mobilenet speed. *Advances in Neural Information Processing Systems*, 35:12934–12949, 2022.

[Li *et al.*, 2024a] Kunchang Li, Xinhao Li, Yi Wang, Yanan He, Yali Wang, Limin Wang, and Yu Qiao. Videomamba: State space model for efficient video understanding. *arXiv preprint arXiv:2403.06977*, 2024.

[Li *et al.*, 2024b] Zhiyuan Li, Tingyu Xia, Yi Chang, and Yuan Wu. A survey of rwkv. *arXiv preprint arXiv:2412.14847*, 2024.

[Liu *et al.*, 2021] Ze Liu, Yutong Lin, Yue Cao, Han Hu, Yixuan Wei, Zheng Zhang, Stephen Lin, and Baining Guo. Swin transformer: Hierarchical vision transformer using shifted windows. In *Proceedings of the IEEE/CVF international conference on computer vision*, pages 10012–10022, 2021.

[Liu *et al.*, 2024a] Jiarun Liu, Hao Yang, Hong-Yu Zhou, Yan Xi, Lequan Yu, Yizhou Yu, Yong Liang, Guangming Shi, Shaoting Zhang, Hairong Zheng, et al. Swinmamba: Mamba-based unet with imagenet-based pre-training. *arXiv preprint arXiv:2402.03302*, 2024.

- [Liu *et al.*, 2024b] Yue Liu, Yunjie Tian, Yuzhong Zhao, Hongtian Yu, Lingxi Xie, Yaowei Wang, Qixiang Ye, and Yunfan Liu. Vmamba: Visual state space model. *arXiv preprint arXiv:2401.10166*, 2024.
- [Long *et al.*, 2014] Jonathan Long, Evan Shelhamer, and Trevor Darrell. Fully convolutional networks for semantic segmentation. *CoRR*, abs/1411.4038, 2014.
- [Paszke *et al.*, 2016] Adam Paszke, Abhishek Chaurasia, Sangpil Kim, and Eugenio Culurciello. Enet: A deep neural network architecture for real-time semantic segmentation. *arXiv preprint arXiv:1606.02147*, 2016.
- [Ruan and Xiang, 2024] Jiacheng Ruan and Suncheng Xiang. Vm-unet: Vision mamba unet for medical image segmentation. *arXiv preprint arXiv:2402.02491*, 2024.
- [Strudel *et al.*, 2021] Robin Strudel, Ricardo Garcia, Ivan Laptev, and Cordelia Schmid. Segmenter: Transformer for semantic segmentation. In *Proceedings of the IEEE/CVF international conference on computer vision*, pages 7262–7272, 2021.
- [Sun *et al.*, 2023] Yutao Sun, Li Dong, Shaohan Huang, Shuming Ma, Yuqing Xia, Jilong Xue, Jianyong Wang, and Furu Wei. Retentive network: A successor to transformer for large language models. *arXiv preprint arXiv:2307.08621*, 2023.
- [Vaswani *et al.*, 2017] Ashish Vaswani, Noam Shazeer, Niki Parmar, Jakob Uszkoreit, Llion Jones, Aidan N Gomez, Łukasz Kaiser, and Illia Polosukhin. Attention is all you need. *Advances in neural information processing systems*, 30, 2017.
- [Xiao *et al.*, 2018] Tete Xiao, Yingcheng Liu, Bolei Zhou, Yuning Jiang, and Jian Sun. Unified perceptual parsing for scene understanding. In *Proceedings of the European conference on computer vision (ECCV)*, pages 418–434, 2018.
- [Xie *et al.*, 2021] Enze Xie, Wenhai Wang, Zhiding Yu, Anima Anandkumar, Jose M Alvarez, and Ping Luo. Segformer: Simple and efficient design for semantic segmentation with transformers. *Advances in neural information processing systems*, 34:12077–12090, 2021.
- [Yang *et al.*, 2023] Gyeongdong Yang, Yungwook Kwon, and Hyunjin Kim. Exmobilevit: Lightweight classifier extension for mobile vision transformer. *arXiv preprint arXiv:2309.01310*, 2023.
- [Yu *et al.*, 2017] Fisher Yu, Vladlen Koltun, and Thomas Funkhouser. Dilated residual networks. In *Proceedings of the IEEE conference on computer vision and pattern recognition*, pages 472–480, 2017.
- [Zhang *et al.*, 2016] Chunjie Zhang, Zhe Xue, Xiaobin Zhu, Huanian Wang, Qingming Huang, and Qi Tian. Boosted random contextual semantic space based representation for visual recognition. *Information Sciences*, 369:160–170, 2016.
- [Zhang *et al.*, 2022] Bowen Zhang, Zhi Tian, Quan Tang, Xiangxiang Chu, Xiaolin Wei, Chunhua Shen, et al. Segvit: Semantic segmentation with plain vision transformers. *Advances in Neural Information Processing Systems*, 35:4971–4982, 2022.
- [Zhang *et al.*, 2023] Haojie Zhang, Yongyi Su, Xun Xu, and Kui Jia. Improving the generalization of segmentation foundation model under distribution shift via weakly supervised adaptation. *arXiv preprint arXiv:2312.03502*, 2023.
- [Zhang *et al.*, 2024a] Songyang Zhang, Ge Ren, Xiaoxi Zeng, Liang Zhang, Kailun Du, Gege Liu, and Hong Lin. Efficient cross-information fusion decoder for semantic segmentation. *Computer Vision and Image Understanding*, 240:103918, 2024.
- [Zhang *et al.*, 2024b] Zhuoyang Zhang, Han Cai, and Song Han. Efficientvit-sam: Accelerated segment anything model without performance loss. *arXiv preprint arXiv:2402.05008*, 2024.
- [Zhao *et al.*, 2017] Hengshuang Zhao, Jianping Shi, Xiaojuan Qi, Xiaogang Wang, and Jiaya Jia. Pyramid scene parsing network. In *Proceedings of the IEEE conference on computer vision and pattern recognition*, pages 2881–2890, 2017.
- [Zheng *et al.*, 2012] Qihua Zheng, Wenqing Li, Weihua Hu, and Guohua Wu. An interactive image segmentation algorithm based on graph cut. *Procedia Engineering*, 29:1420–1424, 2012.
- [Zheng *et al.*, 2021] Sixiao Zheng, Jiachen Lu, Hengshuang Zhao, Xiatian Zhu, Zekun Luo, Yabiao Wang, Yanwei Fu, Jianfeng Feng, Tao Xiang, Philip HS Torr, et al. Rethinking semantic segmentation from a sequence-to-sequence perspective with transformers. In *Proceedings of the IEEE/CVF conference on computer vision and pattern recognition*, pages 6881–6890, 2021.
- [Zhou *et al.*, 2017] Bolei Zhou, Hang Zhao, Xavier Puig, Sanja Fidler, Adela Barriuso, and Antonio Torralba. Scene parsing through ade20k dataset. In *Proceedings of the IEEE conference on computer vision and pattern recognition*, pages 633–641, 2017.
- [Zhu *et al.*, 2023] Guilin Zhu, Runmin Wang, Yingying Liu, Zhenlin Zhu, Changxin Gao, Li Liu, and Nong Sang. An adaptive post-processing network with the global-local aggregation for semantic segmentation. *IEEE Transactions on Circuits and Systems for Video Technology*, 2023.
- [Zhu *et al.*, 2024] Lianghui Zhu, Bencheng Liao, Qian Zhang, Xinlong Wang, Wenyu Liu, and Xinggang Wang. Vision mamba: Efficient visual representation learning with bidirectional state space model. *arXiv preprint arXiv:2401.09417*, 2024.

A Additional results

In this section, we will analyze the experimental results of the proposed Small, Base, and Large models on the ADE20k val, Cityscapes and COCO-Stuff datasets.

A.1 ADE20K

Table 6 summarizes the performance of semantic segmentation models of different scales and architectures on the ADE20K validation dataset. Among smaller models, SenFormer and SegFormer achieved competitive results, but our proposed Small variant outperformed them with an mIoU of 50.7. Moving to models of basic sizes, Swin-B* and Mask2Former stood out, yet our proposed Basic model achieved a strong mIoU of 51.63. In large-scale models, MaskFormer and VMamba-B showed satisfactory results, while our model achieved comparable performance to them.

A.2 Cityscapes

Table 7 provides a detailed showcase of the performance of various models across multiple configurations. Specifically, in the small model category, our Ours-Small model achieves 82.59% and 83.26% in single-scale (mIoU(SS)) and multi-scale (mIoU(MS)) evaluations respectively, surpassing other small-scale models. For the base models, our Ours-Base model achieves 83.17% and 83.8% in mIoU(SS) and mIoU(MS) respectively, outperforming other base models. Ours-Base maintains high performance while keeping relatively moderate computational complexity. In the large model category, our Ours-Large model achieves 83.36% in mIoU(SS), slightly edging out other large models. Although trailing slightly behind Mask2Former (Swin-B*)’s 84.5% in mIoU(MS), Ours-Large boasts a parameter count of 95.81M, demonstrating advantages in parameter and computational efficiency compared to other large models.

A.3 COCO-Stuff

As shown in Table 8, we conducted experiments comparing different model sizes on the COCO-Stuff dataset. The results demonstrate significant advantages of our proposed models (utilizing RMT-S, RMT-B, and RMT-L as backbone networks) in both single-scale and multi-scale scenarios, achieving high average IoU values of 44.32, 45.92, and 45.78 (ss), and 45.48, 46.06, and 46.63 (ms), respectively. In contrast, other models exhibited relatively lower performance in both aspects. In summary, our models have shown outstanding semantic segmentation performance on the COCO-Stuff dataset, showcasing their superiority in terms of accuracy and generalization capabilities.

Method	Backbone	Decoder head	Image Size	#params	mIoU(SS)	mIoU(MS)	FLOPs
SenFormer	Swin-S		512*512	81M	49.2	-	202G
RMT	RMT-S	UperNet	512*512	56M	-	49.8	937G
RMT	RMT-B	FPN	512*512	57M	-	50.4	294G
SegFormer	MiT-B3		512*512	47.3M	49.4	50	79G
VMamba	VMamba-S	UperNet	512*512	76M	49.5	50.5	1037G
VMamba	VMamba-S	UperNet	640*640	76M	50.8	50.8	1620G
MaskFormer	Swin-S		512*512	63M	49.8±0.4	51.0±0.4	79G
SegFormer	MiT-B4		512*512	64.1M	50.31	51.1	95.7G
Ours-Small	RMT-S		512*512	26.52M	50.7	51.29	117.1G
Swin	Swin-B*	UperNet	640*640	121M	-	51.6	471G
SegFormer	MiT-B5		640*640	84.7M	51	51.8	183.3G
RMT	RMT-B	UperNet	512*512	83M	-	52	1051G
Mask2Former	Swin-S		512*512	69M	51.3	52.4	98G
Ours-Base	RMT-B		512*512	53.05M	51.63	52.13	229.66G
SeMask	SeMask Swin-B*	FPN	512*512	96M	49.35	50.98	107G
VMamba	VMamba-B	UperNet	512*512	110M	50	51.3	1167G
RMT	RMT-L	FPN	512*512	98M	-	51.4	482G
MaskFormer	Swin-B		640*640	102M	51.1±0.2	52.3±0.4	195G
Ours-Large	RMT-L		640*640	95.81M	52	52.23	478.54G

Table 6: The results of various model sizes on the ADE20K val. * Indicates pretraining on ImageNet22K.

Method	Backbone	Decoder head	Image Size	#params	mIoU(SS)	mIoU(MS)	FLOPs
Mask2Former	R50		512*1024	44M	79.4	82.2	293G
Mask2Former	R101		512*1024	63M	80.1	81.9	226G
SeMask	SeMask Swin-S	FPN	768*768	56M	77.13	79.14	134G
Mask2Former	Swin-T		512*1024	47M	82.1	83	232G
SegFormer	MiT-B2		1024*1024	27.5M	81	82.2	717.1G
Ours	RMT-S		512*1024	26.52M	82.93	83.52	117.1G
SeMask	SeMask Swin-B*	FPN	768*768	96M	77.7	79.73	217G
SegFormer	MiT-B3		1024*1024	47.3M	81.7	83.3	962.9G
Mask2Former	Swin-S		512*1024	69M	82.6	83.6	313G
Ours	RMT-B		512*1024	53.05M	83.28	83.87	229.66G
SeMask	SeMask Swin-L*	FPN	768*768	211M	78.53	80.39	455G
SegFormer	MiT-B5		1024*1024	84.7M	82.4	84	1460.4G
Mask2Former	Swin-B*		512*1024	107M	83.3	84.5	466G
Mask2Former	Swin-L*		512*1024	215M	83.3	84.3	868G
E CFD-tiny	Swin-Large		512*1024	209M	82.67	83.41	473G
E CFD-small	Swin-Large		512*1024	218M	83.1	83.61	488G
Ours	RMT-L		512*1024	95.81M	83.36	83.91	478.54G

Table 7: The results of various model sizes on the Cityscapes. * Indicates pretraining on ImageNet22K.

Method	Backbone	Decoder head	Image Size	#params	mIoU(SS)	mIoU(MS)
MaskFormer	R101		640*640	-	38.1±0.3	39.8±0.6
MaskFormer	R101c		640*640	-	38.0±0.3	39.3±0.4
SenFormer	R101		512*512	79M	41	42.1
Ours	RMT-S		512*512	26.52M	44.32	45.48
SeMask	SeMask Swin-S	FPN	512*512	56M	40.72	42.27
Ours	RMT-B		512*512	53.05M	45.92	46.06
SeMask	SeMask Swin-B*	FPN	512*512	96M	44.68	46.3
Ours	RMT-L		512*512	95.81M	45.78	46.63

Table 8: The results of various model sizes on the COCO-Stuff. * Indicates pretraining on ImageNet22K.